

## Structural change of the unique-parity $\pi h_{11/2} \otimes \nu h_{11/2}$ configuration in $^{134}\text{Cs}$

H. Pai,<sup>1</sup> G. Mukherjee,<sup>1,\*</sup> A. Raghav,<sup>2</sup> R. Palit,<sup>2</sup> C. Bhattacharya,<sup>1</sup> S. Chanda,<sup>3</sup> T. Bhattacharjee,<sup>1</sup> S. Bhattacharyya,<sup>1</sup> S. K. Basu,<sup>1</sup> A. Goswami,<sup>4</sup> P. K. Joshi,<sup>2</sup> B. S. Naidu,<sup>2</sup> Sushil K. Sharma,<sup>2</sup> A. Y. Deo,<sup>2,†</sup> Z. Naik,<sup>2,‡</sup> R. K. Bhowmik,<sup>5</sup> S. Muralithar,<sup>5</sup> R. P. Singh,<sup>5</sup> S. Kumar,<sup>6</sup> S. Sihotra,<sup>7</sup> and D. Mehta<sup>8</sup>

<sup>1</sup>Variable Energy Cyclotron Centre, 1/AF Bidhan Nagar, Kolkata 700064, India

<sup>2</sup>Department of Nuclear and Atomic Physics, Tata Institute of Fundamental Research, Mumbai-400005, India

<sup>3</sup>Physics Department, Fakir Chand College, Diamond Harbour, West Bengal, India

<sup>4</sup>Saha Institute of Nuclear Physics, Kolkata 700064, India

<sup>5</sup>Inter University Accelerator Centre, New Delhi 110067, India

<sup>6</sup>Department of Physics, Delhi University, New Delhi, India

<sup>7</sup>Department of Physics, Guru Nanak Dev University, Amritsar-143005, India

<sup>8</sup>Department of Physics, Panjab University, Chandigarh-160014, India

(Received 11 July 2011; revised manuscript received 23 August 2011; published 10 October 2011)

A bandlike structure, based on the  $\pi h_{11/2} \otimes \nu h_{11/2}$  configuration, has been identified for the first time in  $^{134}\text{Cs}$  in a gamma-ray spectroscopic study using fusion evaporation reactions. The nature of this band in  $^{134}\text{Cs}$  has been found to be distinctly different than the nearly degenerate doublet rotational band structures, observed in the lighter Cs isotopes for the same configuration. Both the total Routhian surface and the tilted axis cranking calculations were performed to understand the experimental observations. The present results suggest that the  $N = 77$  defines the border of the deformed structure in the  $A \sim 130$  region while approaching  $N = 82$ .

DOI: [10.1103/PhysRevC.84.041301](https://doi.org/10.1103/PhysRevC.84.041301)

PACS number(s): 27.60.+j, 21.10.Pc, 21.10.Re, 23.20.Lv

The nuclei in the  $A \sim 130$  mass region are a rich testing ground for many nuclear symmetries. Many of the nuclei in this region are known to be  $\gamma$  soft and triaxial in nature. Interesting phenomena, such as observation of doublet bands and magnetic rotational (MR) bands which arise due to chiral symmetry breaking and a shears mechanism, respectively, have been observed in many nuclei in this region [1–5]. These occur due to the coupling between the single particle and the collective degrees of freedom in nuclei, with moderate to small deformation. Therefore, both the shape of a nucleus and the position of the Fermi level play important roles in determining the structure of a band. A stable triaxial shape is necessary for the occurrence of the chiral bands and the MR bands are, generally, realized for small deformation [6–8]. A change in the structure of a band, built on a particular configuration, is possible if shape changes from a well-deformed triaxial to a  $\gamma$ -soft one as a function of particle number or angular momentum. However, no such change over has been reported so far in the  $A \sim 130$  region.

For Cs ( $Z = 55$ ) isotopes, the proton and the neutron Fermi surfaces lie near the bottom and the top parts, respectively, of the unique parity  $h_{11/2}$  subshell. The respective orbitals have prolate and oblate shape driving effects. These opposing shape driving effects on a triaxial  $\gamma$ -soft core induce relatively stable triaxial deformation for the odd-odd isotopes of Cs. This manifests in the observation of so-called “chiral bands” in odd-odd Cs isotopes with neutron numbers ranging from

$N = 71$  to  $N = 77$  for the  $\pi h_{11/2} \otimes \nu h_{11/2}$  configuration [5,9,10]. However, as the neutron number increases toward the  $N = 82$  shell closure, it is not clear if the shape driving effects of the neutrons are strong enough to stabilize the triaxial shape and, hence, whether the similar band structure would still persist. Moreover, when approaching the  $N = 82$  shell closure, the potential energy surfaces tend to be  $\gamma$  soft with small deformation. These conditions are ideal for destroying the chiral arrangement and for the emergence of the MR bands.  $^{132}\text{Cs}$  is the heaviest isotope of Cs for which the  $\pi h_{11/2} \otimes \nu h_{11/2}$  configuration was identified, with a rotational band structure along with a possible chiral partner [5]. The above configuration has not yet been identified in  $^{134}\text{Cs}$ . Apart from the low-lying states, studied with  $(n, \gamma)$  and  $(d, p)$  reactions [11,12], there is not much information available on the high spin states in  $^{134}\text{Cs}$ . A few of the high-energy states up to  $\sim 2$  MeV were identified in Ref. [9] but with no spin-parity assignments. We have investigated the high spin states in  $^{134}\text{Cs}$  with the aim, in particular, in studying the nature of the band built on the  $\pi h_{11/2} \otimes \nu h_{11/2}$  configuration, in order to test if the band structure remains unaltered for  $N = 79$ .

The high spin states in  $^{134}\text{Cs}$  were populated by two reactions: (i)  $^{130}\text{Te}(^{11}\text{B}, \alpha 3n)$  at 52 MeV and (ii)  $^{130}\text{Te}(^7\text{Li}, 3n)$  at 30 MeV, carried out at the 14-UD BARC-TIFR Pelletron at Mumbai, India. An array of 8 (7) Compton-suppressed clover Ge detectors, placed in the median plane, was used to detect the gamma rays in the first (second) experiment. The details of the first experiment can be found in Ref. [13]. The trigger conditions in the first and second experiments were optimized for triple- $\gamma$  and double- $\gamma$  coincidences, respectively.  $^{134}\text{Cs}$  was one of the main production channels in the second experiment while it was produced only by an incomplete fusion evaporation reaction in the first.

\* gopal@vecc.gov.in

<sup>†</sup>Present address: Physics Department, University of Massachusetts Lowell, Lowell, MA 01854.

<sup>‡</sup>Present address: School of Physics, Sambalpur University, Jyoti Vihar, Burla, Sambalpur-768019, Orissa, India.

TABLE I. List of  $\gamma$  rays and excited states in  $^{134}\text{Cs}$ , as observed in the present work.

$E_\gamma$ (keV)	$E_i$ (keV)	$J_i^\pi$	$I_\gamma^a$	$R_{\text{DCO}}$ (Err.)	$\Delta$ (Err.)	Multipolarity
88.1(8)	345.1	$7^-$	9.5(8)	0.77(6) <sup>b</sup>	—	$M1 + E2$
127.4(3)	2096.8	$12^+$	15.0(19)	0.72(8) <sup>c</sup>	—	$M1 + E2$
154.6(3)	2251.7	$13^+$	12.2(15)	0.98(13) <sup>b</sup>	—	$M1$
157.3(2)	1551.1	$10^+$	37.2(31)	0.89(7) <sup>b</sup>	—	$M1$
205.7(3)	345.1	$7^-$	10.1(9)	—	—	$M1^e$
205.6(1)	641.1	$8^-$	42.7(35)	0.73(4) <sup>c</sup>	-0.05(6)	$M1 + E2$
211.6(6)	2463.0	$14^+$	4.9(9)	0.86(12) <sup>c</sup>	—	$M1(+E2)$
245.8(4)	257.0	$6^-$	7.4(6)	—	—	$E1^e$
295.9(1)	434.6	$7^-$	53.2(44)	0.75(6) <sup>c</sup>	-0.09(4)	$M1(+E2)$
296.1(4)	641.1	$8^-$	9.4(8)	0.99(5) <sup>b</sup>	-0.18(9)	$M1$
374.6(7)	2345.0	$12^+$	9.7(9)	0.95(12) <sup>c</sup>	—	$M1$
418.5(2)	1969.7	$11^+$	36.4(31)	1.06(11) <sup>c</sup>	-0.24(7)	$M1$
443.8(4)	2788.8	$13^+$	9.1(8)	0.87(11) <sup>c</sup>	—	$M1$
513	3302	( $14^+$ )	—	—	—	—
544.8(2)	2796.2	$14^+$	10.0(16)	0.84(9) <sup>d</sup>	—	$M1 + E2$
609.7(3)	748.3	$9^-$	28.3(23)	0.78(11) <sup>d</sup>	-0.27(8)	$M1$
644.7(3)	1393.8	$9^+$	27.5(23)	0.99(11) <sup>d</sup>	0.32(9)	$E1$
752.7(3)	1393.8	$9^+$	31.6(27)	1.05(13) <sup>b</sup>	0.26(5)	$E1$

<sup>a</sup>Relative  $\gamma$ -ray intensities.

<sup>b</sup>From 245.8-keV ( $E1$ ) DCO gate.

<sup>c</sup>From 752.7-keV ( $E1$ ) DCO gate.

<sup>d</sup>From 154.6-keV ( $M1$ ) DCO gate.

<sup>e</sup>From Refs. [11] and [12].

The coincidence and the intensity relations of the gamma rays were used to construct the level scheme of  $^{134}\text{Cs}$ . For this purpose, an  $E_\gamma$ - $E_\gamma$ - $E_\gamma$  cube and an  $E_\gamma$ - $E_\gamma$  matrix were constructed from the data collected in the first and second experiments, respectively. The spins and parities ( $J^\pi$ ) of the levels were assigned from the deduced multiplicities and the electric and magnetic ( $E$  and  $M$ ) character of the gamma rays deexciting the levels. These were deduced from the measured directional correlation from oriented states ratios ( $R_{\text{DCO}}$ ) [14] and integrated polarization asymmetry (IPDCO) ratios [15,16], respectively. Data collected only from the second experiment were used for the  $R_{\text{DCO}}$  and the IPDCO ratio analysis. An angle-dependent ( $90^\circ$  vs  $145^\circ$ )  $E_\gamma$ - $E_\gamma$  matrix was constructed for  $R_{\text{DCO}}$ . For the IPDCO analysis, the data from the  $90^\circ$  detectors were used. The validity of the methods of the DCO and the IPDCO measurements were checked from the known transitions in  $^{133}\text{Cs}$  [17], which were also produced in the second experiment. The  $\gamma$ -ray energies, their  $R_{\text{DCO}}$  and IPDCO ( $\Delta$ ) values, deduced multiplicities, level energies and  $J^\pi$  assignment of the excited levels in  $^{134}\text{Cs}$  are given in Table I.

Figure 1 shows the partial level scheme of  $^{134}\text{Cs}$  obtained in the present work. Most of the low-energy part of this level scheme (below the 435-keV level) has been adopted from earlier works [11,12]. The coincidence correlations among the gamma rays have been deduced by putting gates (single and double) on several known gamma rays in  $^{134}\text{Cs}$ . Representative single-gated and a sum of double-gated gamma ray spectra are shown in Figs. 2(a) and 2(b), respectively. The high spin states have been extended up to  $J^\pi = (14^+)$  and 3.3 MeV in the excitation energy in the present work.

A  $9^+$  state is known in all the lighter odd-odd Cs isotopes ( $A = 126$ – $132$ ) corresponding to the  $\pi h_{11/2} \otimes \nu h_{11/2}$  configuration [9]. This state in  $^{134}\text{Cs}$  has been identified and characterized for the first time in this work. By gating on the previously known pure dipole ( $E1$ ) transition of 246 keV [11], the 296-keV (from the 641-keV level) and the 753-keV

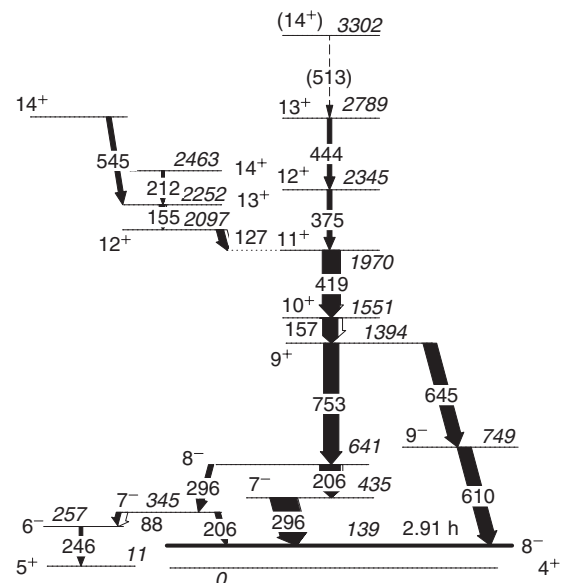


FIG. 1. Partial level scheme of  $^{134}\text{Cs}$ , as obtained from the present work. The low-lying states up to 435 keV are mostly adopted from the earlier works [11,12].

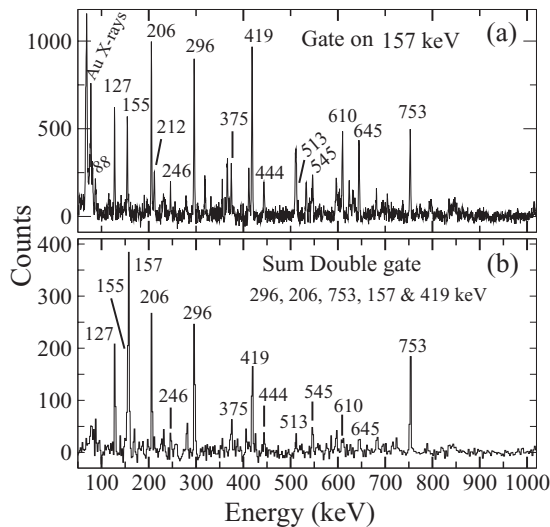


FIG. 2. (a) Single-gated and (b) sum of double-gated spectra of  $^{134}\text{Cs}$  showing the  $\gamma$  rays in the level scheme presented in Fig. 1. The unmarked peaks are the contaminants.

gamma rays were found to be  $M1$  and  $E1$ , respectively, from their measured DCO ratio ( $\sim 1$ ) and the negative and positive values of the IPDCO ratios (see Table I). The spin parity of the 345-keV level was known to be  $7^-$  [11]. Therefore, the spin parity of the 641- and 1394-keV levels are identified as  $8^-$  and  $9^+$ , respectively. The low-lying negative parity states in  $^{134}\text{Cs}$  were interpreted as the  $\nu h_{11/2}$  coupled to  $\pi d_{5/2}$  or  $\pi g_{7/2}$  [11]. An  $E1$  transition (753 keV), between one of these states and the  $9^+$  band head, indicates that there is a change in configuration which must involve a change in parity. The spin, parity, and the excitation energy of the state at 1394 keV favor a change in proton configuration from  $d_{5/2}$  (or  $g_{7/2}$ ) to  $h_{11/2}$ . The band-head spins of the  $\pi h_{11/2} \otimes \nu h_{11/2}$  configuration in the lighter odd-odd Cs isotopes are  $9^+$ . The energy of this  $9^+$  state in  $^{134}\text{Cs}$  smoothly extends the systematic of the variation of the band-head energies of the  $\pi h_{11/2} \otimes \nu h_{11/2}$  configuration in an isotopic chain. Our assignment of the 1394-keV,  $9^+$  state in  $^{134}\text{Cs}$  as the band head of the above configuration is supported by this smooth variation, as prescribed by Liu *et al.* [18].

The DCO values of the gamma rays, in the band built on this  $9^+$  band head, indicate that these are predominantly dipole in nature. The  $M1$  nature of the 419-keV gamma ray is evident from the negative value of its IPDCO ratio. The IPDCO ratios could not be obtained for the other gamma rays in this band for either their energies or intensities are too low. However, as these transitions are in band with the 419-keV gamma ray, the 157-, 375-, 444-, and (513)-keV gamma rays are considered to be  $M1$ .

The above bandlike structure in  $^{134}\text{Cs}$  looks distinctly different in nature, compared to the bands built on the same configuration in other lighter isotopes of Cs [9]. This band in  $^{134}\text{Cs}$  does not have the features of a well-developed rotational band with  $E2$  crossover transitions, as observed in the lighter isotopes. A side band observed in the lighter isotopes, which was interpreted as the so-called ‘‘chiral partner band,’’ has not been observed in  $^{134}\text{Cs}$ . The features of the levels in this dipole band have been compared with the general

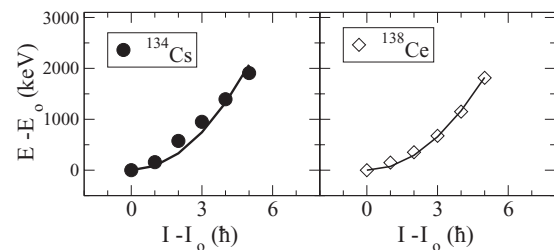


FIG. 3. Relative energy vs spin curves for the band built on the  $9^+$  band head for  $^{134}\text{Cs}$  (left-hand side) and for a known MR band in  $^{138}\text{Ce}$  (right-hand side). The fitted curves are shown by the solid lines (see the text for details).

criteria of a MR band [8,19]. For the MR bands, the level energies ( $E$ ) and the spins ( $I$ ) in the band follow the pattern  $E - E_0 \sim A_0 * (I - I_0)^2$ , where  $E_0$  and  $I_0$  are the energy and spin of the band head, respectively, and  $A_0$  is a constant. The plot of  $E - E_0$  vs  $I - I_0$  is shown in Fig. 3 for the above band in  $^{134}\text{Cs}$  and a known MR band of  $^{138}\text{Ce}$  [4] in this region. The two plots look very similar. The solid lines in this figure are the fitting of the data using the above relation.

The good fitting for the transitions in  $^{134}\text{Cs}$  indicates a bandlike structure. Considering the upper limit of the intensities of the unobserved, crossover transitions as the level of the background in our data, the lower limit of the  $B(M1)/B(E2)$  ratio has been estimated to be  $> 18\mu^2/(eb)^2$ . This compares well with the typical value of  $\geq 20\mu^2/(eb)^2$  for a MR band. The dynamic moment of inertia  $J^{(2)} \sim 16\hbar^2 \text{ MeV}^{-1}$  obtained for this band in  $^{134}\text{Cs}$  is also within the typical value of  $J^{(2)} \sim 10\text{--}25\hbar^2 \text{ MeV}^{-1}$  for a MR band. All these indicate that the above band is most likely a MR band. This band is crossed by another band above  $11^+$ , which subsequently becomes yrast, whose configuration has been tentatively identified as  $\pi g_{7/2} \otimes \nu g_{7/2} h_{11/2}^2$  from the systematics of odd-odd Cs isotopes. The small irregularity in the band around this spin value seems to be because of the interaction between the two bands. Such irregularities are, however, not uncommon for the suggested MR bands in this region [20].

The experimental observations clearly indicate that the structure of the band built on the  $\pi h_{11/2} \otimes \nu h_{11/2}$  configuration, in odd-odd Cs isotopes, has been changed quite drastically from a more regular collective rotational band which resembles chiral doublet bands for  $N < 79$  to a bandlike structure which resembles a MR band for  $N = 79$ . The quadrupole deformation ( $\beta_2$ ) and the  $\gamma$  softness plays important roles in determining the methods of generation of the angular momentum in a nucleus. Chiral symmetry breaking is best realized in a stable triaxially deformed nucleus while MR dominates in a near spherical nucleus. Large amounts of  $\gamma$  softness can destroy the chiral symmetry, while for large  $\beta_2$  the quadrupole rotation dominates over magnetic rotation. In order to understand the difference in the observed band structures, the shapes of the odd-odd Cs isotopes in the  $\pi h_{11/2} \otimes \nu h_{11/2}$  configuration have been studied by calculating the total Routhian surfaces (TRSs). The Hartree-Fock-Bogoliubov code of Nazarewicz *et al.* [21,22] was used for the calculations. The procedure has been outlined in Refs. [23] and [24]. A deformed Woods-Saxon potential and pairing interaction was used

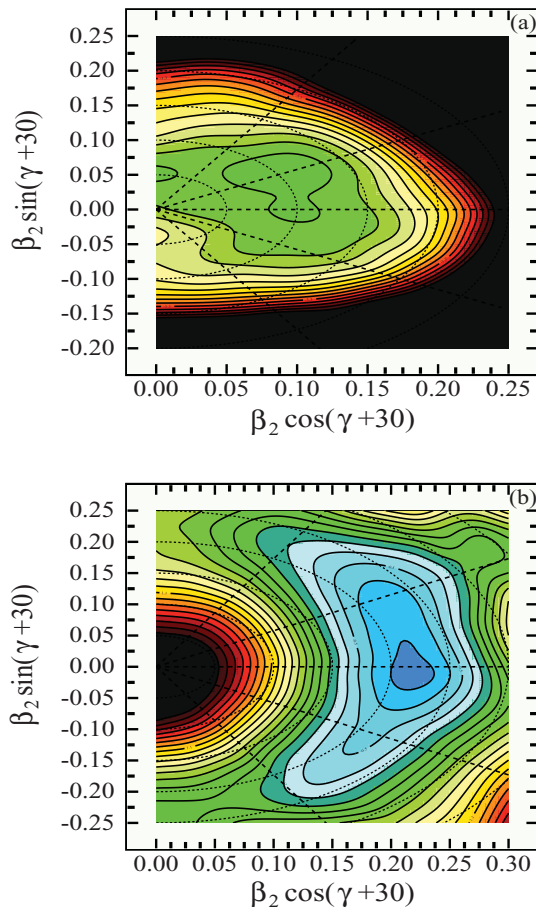


FIG. 4. (Color online) Contour plots of the total Routhian surfaces (TRSs) in the  $\beta_2$ - $\gamma$  deformation mesh for the  $\pi h_{11/2} \otimes \nu h_{11/2}$  configuration calculated at a rotational frequency  $\hbar\omega = 0.2$  MeV in  $^{134}\text{Cs}$  (a) and in  $^{126}\text{Cs}$  (b). The contours are 150 keV apart.

with the Strutinsky shell corrections method. The TRS were calculated in the  $\beta_2$ - $\gamma$  deformation mesh points and minimized in the hexadecapole deformation  $\beta_4$ . The representative contour plots of the TRSs are shown in Fig. 4 for  $^{126}\text{Cs}$  and  $^{134}\text{Cs}$  in the  $\pi h_{11/2} \otimes \nu h_{11/2}$  configuration.

In these plots,  $\gamma = 0^\circ$  ( $\gamma = -60^\circ$ ) corresponds to the prolate (oblate) shape. For a triaxial shape,  $\gamma$  is in between these values and  $\gamma = \pm 30^\circ$  corresponds to the maximum of triaxiality. Figure 4 shows that the  $\gamma$  softness is much larger for heavier isotope  $^{134}\text{Cs}$  than in  $^{126}\text{Cs}$ , for which a stable triaxial minimum is realized.

The variation in the TRS energies  $E_{\text{TRS}}$  (relative to the minimum) for the above configuration is shown in Fig. 5 as a function of the triaxiality parameter  $\gamma$  for the odd-odd Cs isotopes. The  $\beta_2$  values (shown in the inset as a function of mass number  $A$ ) for these were kept close to the minimum of the TRS.

It can be seen from Fig. 5 that  $^{126}\text{Cs}$  has a minimum close to  $\gamma \sim -30^\circ$ . As the neutron number increases, another minimum near  $\gamma \sim -90^\circ$  appears. The two minima, however, are separated by a well-defined barrier which vanishes for the neutron-rich isotopes of  $^{134}\text{Cs}$  and  $^{136}\text{Cs}$ . In other words, while there are stable triaxial shapes for lighter isotopes, the energy

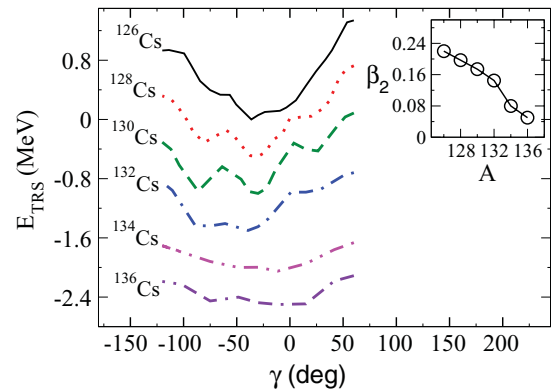


FIG. 5. (Color online) The calculated TRS energies  $E_{\text{TRS}}$  (relative to the minimum) as a function of the triaxiality parameter  $\gamma$  for the odd-odd Cs isotopes in the  $\pi h_{11/2} \otimes \nu h_{11/2}$  configuration. An offset is given to each plot for clarity. The calculated values of the deformation  $\beta_2$ , obtained from the minimum of the TRS, are shown in the inset for those isotopes.

surfaces become more and more  $\gamma$  soft as the neutron number increases. It is also observed from the inset that  $\beta_2$  decreases gradually for the heavier isotopes, which is expected as the neutron number approaches the  $N = 82$  shell closure.

The stable triaxial deformation, together with the relatively large  $\beta_2$  value (between 0.22 and 0.15), favors the regular collective rotational-like structure to dominate for  $^{126-132}\text{Cs}$ , as has been reported [9]. On the other hand,  $^{134,136}\text{Cs}$  are very  $\gamma$  soft and  $\beta_2 < 0.1$ . The lack of substantial quadrupole deformation is reflected in the absence of  $E2$  transitions in  $^{134}\text{Cs}$ . Moreover, as the neutron number increases, the neutron Fermi level moves toward the upper part of the  $h_{11/2}$  subshell and neutron holes are created in the high- $\Omega$  orbital. These are

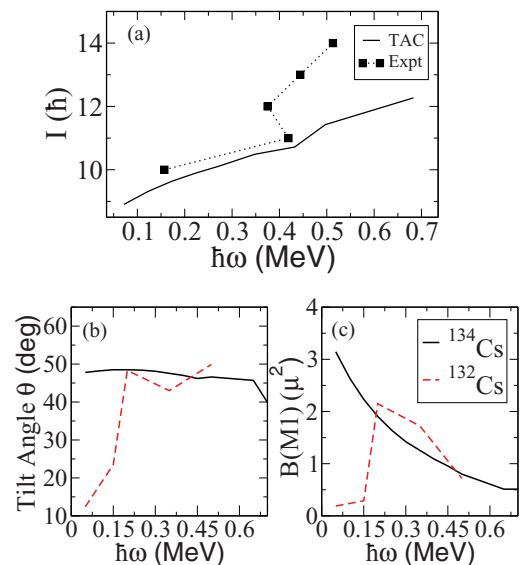


FIG. 6. (Color online) Results of the TAC calculations for the  $\pi h_{11/2} \otimes \nu h_{11/2}$  bands in  $^{132,134}\text{Cs}$ . (a) Experimental and calculated plots of frequency ( $\hbar\omega$ ) vs spin ( $I$ ) for  $^{134}\text{Cs}$ . (b) and (c) Tilt angle and  $B(M1)$  values as a function of  $\hbar\omega$  for  $^{134}\text{Cs}$  (solid line) and  $^{132}\text{Cs}$  (dashed line).

favorable conditions for the onset of the shears mechanism in  $^{134,136}\text{Cs}$ . A band structure similar to  $^{134}\text{Cs}$  is expected in  $^{136}\text{Cs}$  as well.

The tilted axis cranking (TAC) calculations [6,25,26] have been carried out for the  $\pi h_{11/2} \otimes \nu h_{11/2}$  configuration in  $^{134}\text{Cs}$  and  $^{132}\text{Cs}$ . The planar hybrid version of the TAC was used for the calculations. The procedure has been outlined in Refs. [20] and [27]. The Woods-Saxon potential, with universal parameters, was also used in these calculations. The pairing parameters for protons and neutrons were chosen as 80% of the odd-even mass difference. These calculations produce a minimum at a deformation of  $\epsilon_2 = 0.072$  for  $^{134}\text{Cs}$ , in good agreement with the TRS calculations. Figure 6 shows the results of the TAC calculations. The experimental and calculated plots of cranking frequency  $\hbar\omega$  versus spin ( $I$ ) for the above band in  $^{134}\text{Cs}$  [Fig. 6(a)] have reasonably good agreement for the lower spin states before the band crossing. An average tilt angle of  $\theta = 48.3^\circ$  is obtained for  $^{134}\text{Cs}$  in the TAC calculations, which remains remarkably constant throughout the band, as shown in Fig. 6(b). The calculated  $B(M1)$  values for  $^{134}\text{Cs}$  decrease with frequency, as shown in Fig. 6(c), which is a typical characteristic of a shears (MR) band. However, the calculations for  $^{132}\text{Cs}$ , shown also in Figs. 6(b) and 6(c) (dotted lines), show contrasting behaviors, at least at the lower frequencies. Therefore, the TAC calculations clearly suggest that the  $\pi h_{11/2} \otimes \nu h_{11/2}$  band in  $^{134}\text{Cs}$  behaves differently than its immediate odd-odd neighbor  $^{132}\text{Cs}$ . Hence, it may be concluded that there is a change of character of the  $\pi h_{11/2} \otimes \nu h_{11/2}$  configuration at

$N = 79$  for the odd-odd Cs isotopes, which can be understood as a change in shape from both the TRS and the TAC calculations.

In summary, the high spin level structure of  $^{134}\text{Cs}$  has been investigated by heavy-ion-induced fusion evaporation reactions. The  $\pi h_{11/2} \otimes \nu h_{11/2}$  band has been identified and characterized for the first time in  $^{134}\text{Cs}$ . The present experimental observations indicate that the structure of the band built on this configuration for  $^{134}\text{Cs}$  is distinctly different from its lighter odd-odd isotopes. The nearly degenerate rotational doublet band structure, observed for the lighter odd-odd isotopes of Cs, does not persist in the  $N = 79$  isotope  $^{134}\text{Cs}$ . The TRS and the TAC calculations support the observed change in the band structure. The TAC calculations indicate a possible MR nature for this configuration in  $^{134}\text{Cs}$ , in sharp contrast to  $^{132}\text{Cs}$ . The results suggest that the  $N = 77$  defines the border of the well-deformed structure in  $A \sim 130$  region while approaching  $N = 82$ , as was the conjecture of Ref. [5]. However, to establish the explicit nature of this change, in particular a possible transition from an aplanar configuration for  $N < 79$  to a planar configuration for  $N \geq 79$ , more experimental work and detailed three-dimensional TAC calculations are needed.

The authors are thankful to the BARC-TIFR pelletron operators for providing good beams, and to S. S. Ghugre and N. S. Pattabiraman for their help during the first experiment. This work was partially funded by the D.S.T., Government of India (No. IR/S2/PF-03/2003-I).

- 
- [1] K. Starosta *et al.*, *Nucl. Phys. A* **682**, 375c (2001).  
 [2] C. M. Petrache *et al.*, *Z. Phys. A* **344**, 227 (1992); *Nucl. Phys. A* **597**, 106 (1996).  
 [3] C. W. Beausang *et al.*, *Nucl. Phys. A* **682**, 394c (2001).  
 [4] T. Bhattacharjee *et al.*, *Nucl. Phys. A* **825**, 16 (2009).  
 [5] G. Rainovski *et al.*, *Phys. Rev. C* **68**, 024318 (2003).  
 [6] S. Frauendorf, *Rev. Mod. Phys.* **73**, 463 (2001).  
 [7] H. Hubel, *Prog. Part. Nucl. Phys.* **54**, 1 (2005).  
 [8] R. M. Clark and A. O. Macchiavelli, *Annu. Rev. Nucl. Part. Sci.* **50**, 1 (2000).  
 [9] T. Koike, K. Starosta, C. J. Chiara, D. B. Fossan, and D. R. LaFosse, *Phys. Rev. C* **67**, 044319 (2003).  
 [10] S. Wang, Y. Liu, T. Komatsubara, Y. Ma, and Y. Zhang, *Phys. Rev. C* **74**, 017302 (2006).  
 [11] M. Bogdanovic *et al.*, *Nucl. Phys. A* **470**, 13 (1987).  
 [12] V. L. Alexeev *et al.*, *Nucl. Phys. A* **248**, 249 (1975).  
 [13] T. Bhattacharjee *et al.*, *Nucl. Phys. A* **750**, 199 (2005); S. Chanda *et al.*, *ibid.* **775**, 153 (2006).  
 [14] A. Krämer-Flecken *et al.*, *Nucl. Instrum. Methods Phys. Res., Sect. A* **275**, 333 (1989).  
 [15] K. Starosta *et al.*, *Nucl. Instrum. Methods Phys. Res. Sect. A* **423**, 16 (1999).  
 [16] R. Palit *et al.*, *Pramana* **54**, 347 (2000).  
 [17] U. Garg, T. P. Sjoreen, and D. B. Fossan, *Phys. Rev. C* **19**, 207 (1979).  
 [18] Y. Liu *et al.*, *Phys. Rev. C* **58**, 1849 (1998); Y. Liu, Y. Ma, S. Zhou, and H. Zheng, *ibid.* **54**, 719 (1996).  
 [19] A. K. Jain *et al.*, *Pramana* **75**, 51 (2010).  
 [20] S. Kumar *et al.*, *Phys. Rev. C* **76**, 014306 (2007).  
 [21] W. Nazarewicz *et al.*, *Nucl. Phys. A* **512**, 61 (1990).  
 [22] W. Nazarewicz *et al.*, *Nucl. Phys. A* **435**, 397 (1985).  
 [23] G. Mukherjee *et al.*, *Phys. Rev. C* **64**, 034316 (2001).  
 [24] G. Mukherjee *et al.*, *Nucl. Phys. A* **829**, 137 (2009).  
 [25] S. Frauendorf, *Nucl. Phys. A* **557**, 259c (1993).  
 [26] S. Frauendorf, *Nucl. Phys. A* **667**, 115 (2000).  
 [27] P. Agarwal *et al.*, *Phys. Rev. C* **76**, 024321 (2007).